Theory of the Three-Dimensional Quantum Hall Effect in Graphite

B. Andrei Bernevig,[1] Taylor L. Hughes,[2] Srinivas Raghu,[2] and Daniel P. Arovas[2,3]

[1]*Princeton Center for Theoretical Physics, Princeton University, Princeton, New Jersey 08544, USA*
[2]*Department of Physics, Stanford University, Stanford, California 94305, USA*
[3]*Department of Physics, University of California at San Diego, La Jolla, California 92093, USA*

(Received 22 February 2007; published 4 October 2007)

We predict the existence of a three-dimensional quantum Hall effect plateau in a graphite crystal subject to a magnetic field. The plateau has a Hall conductivity quantized at $\frac{4e^2}{\hbar}\frac{1}{c_0}$ with c_0 the c-axis lattice constant. We analyze the three-dimensional Hofstadter problem of a realistic tight-binding Hamiltonian for graphite, find the gaps in the spectrum, and estimate the critical value of the magnetic field above which the Hall plateau appears. When the Fermi level is in the bulk Landau gap, Hall transport occurs through the appearance of chiral surface states. We estimate the magnetic field necessary for the appearance of the effect to be 15.4 T for electron carriers and 7.0 T for holes.

DOI: 10.1103/PhysRevLett.99.146804 PACS numbers: 73.43.−f, 71.70.Di

Recent advances in the fabrication of single graphene sheets as well as the striking initial experiments on the relativistic quantum Hall effect in graphene [1,2] have generated intense interest in this remarkable material. Most of the theoretical and experimental research has focused on the properties of the low energy excitations close to half filling which have a Dirac spectrum with a speed of light of the order of 10^6 m/s. The spin-unpolarized quantum Hall effect shows a sequence of plateaus at $\sigma_{xy} = (n + \frac{1}{2}) \times 4\frac{e^2}{h}$ consistent with the existence of two Dirac cones as well as a spin degeneracy [1,2].

The phenomenon of Hall conductivity quantization is, however, not restricted to two dimensions and can occur in bulk samples, albeit under more stringent conditions. It was first observed by Halperin [3] that for a three-dimensional (3D) electron system in a periodic potential, if the Fermi level lies inside an energy gap, the conductivity tensor is necessarily of the form:

$$\sigma_{ij} = \frac{e^2}{2\pi h}\epsilon_{ijk}G_k, \tag{1}$$

where ϵ_{ijk} is the fully antisymmetric tensor and $\vec{G}$ (which may be zero) is a reciprocal lattice vector. With the exception of engineered multiquantum well systems [4], the three-dimensional quantum Hall effect (3DQHE) has been observed only in the Bechgaard salts [5,6], where a density wave forms due to in-plane anisotropy. These materials are highly 2D, with hopping ratios $t_x{:}t_y{:}t_z \approx 1{:}0.1{:}0.003$. The c-axis hopping is always neglected.

By contrast, in graphite the effective in-plane nearest-neighbor hopping is $t_\parallel \simeq 3.16$ eV and the c-axis hopping $t_\perp \simeq -0.39$ eV [7]. Indeed, were the graphene sheets in graphite stacked directly atop one another ($\alpha\alpha\alpha\alpha$ stacking), the dispersion in an external field would be $E_n(B, k_z) = -2t_\perp \cos(k_z c_0) - \mathrm{sgn}(n)\sqrt{|n|B/B_0}\,t_\parallel$, with $B_0 = (hc/e)/3\pi a_0^2 = 7275$ T. The c-axis dispersion would then overwhelm the Landau gaps for fields below $B^* = (4t_\perp/t_\parallel)^2 B_0 \approx 1800$ T, which is unattainably large. This is typically the scenario in layered materials, even when the hopping anisotropy is as large as 10:1.

In this Letter we show that a true bulk room-temperature 3DQHE is realized in *doped* graphite under a large magnetic field parallel to the c axis. Three factors conspire to render this possible: the large Landau gap of the integer quantum Hall state in graphene, the weak interplane hopping, and especially the Bernal stacking. We first give a physical argument for the existence of 3DQHE based on adiabatic continuity, then perform a full Hofstadter calculation [8] in 3D of the band and surface state structure, using the realistic Johnson-Dresselhaus [9] Hamiltonian for graphite, plus a magnetic field. We find the minimum magnetic field necessary for a 3DQHE to be 15.4 T for electrons and 7.0 T for holes, and show that only *one* Hall plateau (Fig. 1) will be observed due to band closing in the higher Landau levels (LLs). Beside the obvious prediction of a plateau in off-diagonal conductive response, we also predict that a correlated chiral surface state [10] occurs at the boundary of the sample. Based on the recent experimental focus on graphite [11] we believe our prediction is testable with current experimental techniques. Previous Hall plateaus observed in *undoped* graphite [12,13] are even in B and come in multiple sequences consistent with the graphene QHE plateaus [1,2]. They are hence different than our prediction of a *single* quantized Hall plateau of Hall conductivity twice as large as the one observed in graphene for Fermi level in the first Landau gap of *doped* graphite.

Graphite is a layered material consisting of weakly coupled graphene layers in an $\alpha\beta\alpha\beta$ configuration known as Bernal stacking [14], as depicted in Fig. 1 [15]. If we "turn off" the interlayer hopping, then in a field each layer exhibits a relativistic QHE as previously described, with a LL energy $E_n = \pm\sqrt{2n}\hbar v/\ell$, where $\ell = \sqrt{\hbar c/eB}$ is the magnetic length, $n = 0, 1, \ldots$, and $v \approx 10^6$ m/s. Typical values of the gap are roughly 0.1 eV for $B = 10$ T and >0.25 eV for $B > 40$ T, thus making graphene the first

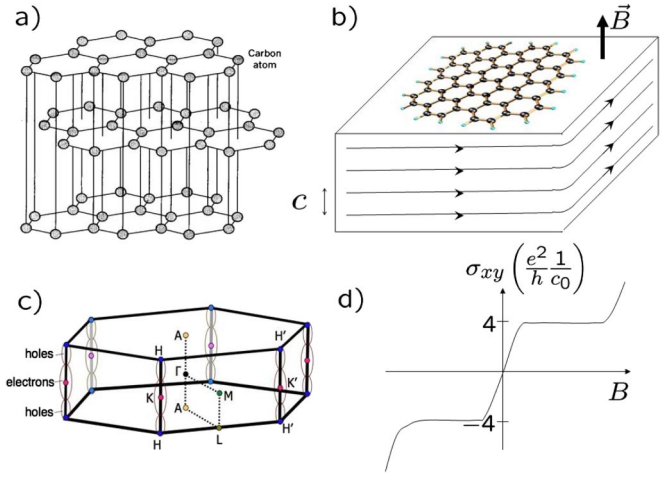

FIG. 1 (color online). (a) Graphite in Bernal stacking. (b) Under strong magnetic field, graphite is gapped in the bulk and exhibits chiral surface sheet states. (c) Idealized Brillouin zone for graphite. (d) Predicted 3D Hall conductivity, quantized in units of $1/c_0$. Only one plateau is observable in graphite.

system to exhibit quantized Hall conductance at room temperature. Placing the Fermi level in the first Landau gap, the uncoupled graphene layers trivially exhibit a 3DQHE, with the bulk enveloped by a sheath of chiral surface states as in Fig. 1. Adiabatically reintroducing the intralayer hopping causes almost all the LLs to disperse with k_z. The exceptions are the zero modes, which are stable in an idealized model due to particle-hole symmetry, as we show below. By adiabatic continuity, the sheath of chiral states (and hence the 3DQHE) must be stable as long as the Landau gap does not collapse.

We first show that the statement above is true for a simplified toy model of graphite. If we introduce a parameter $x = t_\perp/t_\perp^{\text{graphite}}$ which interpolates between uncoupled graphene layers ($x = 0$) and graphite ($x = 1$), the minimal Hamiltonian of our system is a 4×4 Hermitian matrix acting on the lattice spinor $(\psi_A, \psi_B, \psi_C, \psi_D)$, where (A, B) and (C, D) are the two inequivalent sites of the lower and upper graphene layers in the Bernal stacking, respectively. Its nonzero independent elements are $\mathcal{H}_{AB} = -\mathcal{H}^*_{CD} = \frac{\sqrt{3}}{2} t_\parallel a_0 k_-$, and $\mathcal{H}_{AC} = -2t_\perp \cos(\frac{1}{2} k_z c_0)$. The in-plane hopping is $t_\parallel = 3.16$ eV, $t_\perp = 0.39$ eV is the interlayer (A-C) hopping in graphite ($x = 1$) [14], and $a_0 = 2.456$ Å is the graphene lattice constant (in-plane A-A distance). The c-axis lattice constant is $c_0 = 6.74$ Å, and $k_\pm = k_x \pm i k_y$. The in-plane dispersion is expanded about the point $K = (\frac{4\pi}{3a_0}, 0, 0)$, which is the Dirac point in graphene. In a uniform magnetic field, adopting the gauge $\vec{A} = \frac{1}{2} B(-y, x, 0)$, the Kohn-Luttinger substitution $k_\pm \to k_x \pm i k_y + \frac{e}{\hbar c}(A_x \pm i A_y)$ [16]. When $x = 1$, this is the model used in [17]. Let $b^\dagger$, b be LL creation and annihilation operators (with $[b, b^\dagger] = 1$), and introduce the notation $c_z = \cos(\frac{1}{2} k_z c_0)$. The Hamiltonian is

$$\mathcal{H}(x) = \begin{pmatrix} 0 & -\epsilon t_\parallel b & -2t_\perp c_z & 0 \\ -\epsilon t_\parallel b^\dagger & 0 & 0 & 0 \\ -2t_\perp c_z & 0 & 0 & -\epsilon t_\parallel b^\dagger \\ 0 & 0 & -\epsilon t_\parallel b & 0 \end{pmatrix} \quad (2)$$

with $\epsilon = B/B_0$. Diagonalizing in the basis $\psi = (|n\rangle, |n+1\rangle, |n\rangle, |n-1\rangle)$, for $n > 0$, one finds the eigenvalues

$$E_n = \pm[(n + \tfrac{1}{2})\epsilon^2 t_\parallel^2 + 2t_\perp^2 c_z^2 \pm \sqrt{\tfrac{1}{4}\epsilon^4 t_\parallel^4 + 4(n + \tfrac{1}{2})\epsilon^2 t_\parallel^2 t_\perp^2 c_z^2 + 4t_\perp^4 c_z^4}]^{1/2}. \quad (3)$$

This spectrum has explicit particle-hole symmetry. For $n = 0$ there are eigenvalues at $\pm(\epsilon^2 t_\parallel^2 + 4t_\perp^2 c_z^2)^{1/2}$ and a doubly degenerate level at $E_0 = 0$. (All levels receive an additional double degeneracy owing to the existence of the inequivalent K point.) The next Landau bands are the lowest two energy levels of $n = 1$. We observe that the gap between the zero mode and the proximate LLs cannot collapse upon interpolating between $x = 0$ and $x = 1$ for *any* value of the magnetic field. By adiabatic continuity, then, the Hall conductance when the Fermi level is in the 3D gap (with doubling for spin) is

$$\sigma_{xy} = \frac{4e^2}{h} \int \frac{d^3k}{(2\pi)^3} \operatorname{Im} \left\langle \frac{\partial \psi}{\partial k_x} \middle| \frac{\partial \psi}{\partial k_y} \right\rangle = (2n+1)\frac{4e^2}{h} \int \frac{dk_z}{2\pi} = (2n+1)\frac{4e^2}{hc_0}. \quad (4)$$

With the Fermi level between the zero mode and the first LL, $n = 0$ and $\sigma_{xy} = \pm 4e^2/hc_0$. The Bernal stacking of graphite accounts for the extra factor of 2 relative to graphene and $\int \frac{d^2k}{(2\pi)^2} \operatorname{Im}\langle \partial_{k_x}\psi | \partial_{k_y}\psi \rangle = 2n + 1$ is the TKNN integer [18] of the relativistic graphene bands when the Fermi level is placed in the nth bulk gap. We

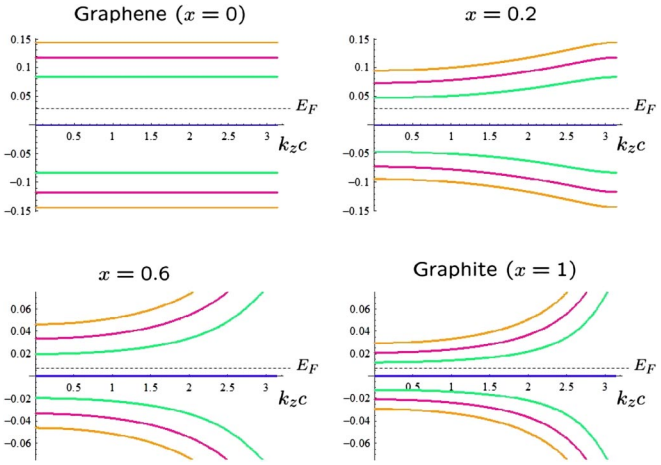

FIG. 2 (color online). Zero mode spectrum and Landau levels of our toy model in $B = 10$ T interpolated between graphene ($x = 0$), with no k_z dispersion, and graphite ($x = 1$). The zero mode (blue line) is doubly degenerate, giving a 3D Hall conductance of $\frac{e^2}{h}\frac{1}{c_0}$ per independent K point per spin.

TABLE I. Tight-binding parameters

Parameter	meV	Parameter	meV	Parameter	meV
$t_{AB}^{\parallel,1} = t_{CD}^{\parallel,1}$	4200	$t_{AB}^{\parallel,2} = t_{CD}^{\parallel,2}$	512.5	$t_{AB}^{\parallel,3} = t_{CD}^{\parallel,3}$	15
t_{AC}	−390	t_{BD}	−315	$t_{AD} = t_{BC}$	−44
$t_{AA'}^{\perp} = t_{CC'}^{\perp}$	−19	$t_{BB'}^{\perp} = t_{DD'}^{\perp}$	10	Δ	50

observe that the gap between the first and the second LL in graphite closes for any realistic value of the B field (Fig. 2), and hence higher n plateaus will not be observed. Zeeman splitting could give rise to a $\sigma_{xy} = 0$ plateau, but it is smeared by the dispersion of the zero mode in the realistic graphite model used below, and hence the predicted Hall conductance is sketched in Fig. 1.

The existence of a full gap in the 3D LL spectrum is an artifact of the toy model involving only $t_{\parallel}$ and $t_{\perp}$. It derives from the presence of a flat twofold degenerate band at the Fermi level along the H-K spines of Brillouin zone [Fig. 1(c)] and the Bernal stacking. More realistic treatments, such as the Slonczewski-Weiss-McClure (SWMC) [7] or Johnson-Dresselhaus (JD) [9] models, contain small c-axis B-B (D-D) hopping terms, through the open hexagons of the CD (AB) plane. Their value is small on the scale of nearest-neighbor hopping—only 10 meV, leading to a bandwidth of 40 meV along the H-K spine. But the presence of such terms is crucial toward understanding the properties of graphite. At $B = 0$, they result in semimetallic behavior, whereas the toy model incorrectly predicts a zero gap semiconductor. For weak fields, they lead to overlap of the LLs and destruction of the QHE. However, as we shall show, the principal gaps surrounding the central $n = 0$ LLs survive for $B > 7.0$ T (holes) and $B > 15.4$ T

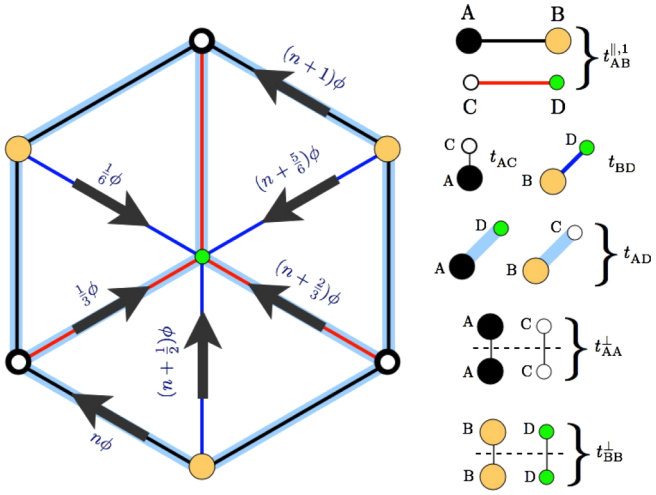

FIG. 3 (color online). Hopping matrix elements and flux assignment. Sites A and B belong to different graphene layers than C and D. Bernal stacking corresponds to A and C differing by a c-axis translation. Not shown are further-neighbor in-plane hoppings $t_{AB}^{\parallel,2}$ and $t_{AB}^{\parallel,3}$. $\phi = 2\pi p/q$ is the magnetic flux per hexagon in units of $\hbar c/e$, and n runs from 1 to q the size of the magnetic unit cell.

(particles). Lightly doped graphite, then, will exhibit a 3DQHE at these fields. We next describe our solution of the JD model in a magnetic field on a torus and a Laughlin cylinder, finding the LLs and the surface states, and determining the critical fields B_c at which energy gaps open across the entire Brillouin zone [19,20].

The JD model [9] is a tight-binding Hamiltonian derived from the $\mathbf{k} \cdot \mathbf{p}$ theory of SWMC. Its nine parameters are given in Table I. In addition to nearest-neighbor hoppings, there are also further-neighbor hoppings, both in-plane (extending to third and fourth neighbor) and between planes. There is also an energy asymmetry $\Delta = \varepsilon_{A(C)} - \varepsilon_{B(D)}$. We introduce a magnetic field via Peierls phases on the links, preserving all rotational (and screw axis) symmetries of the lattice, as in Fig. 3.

We solve the model through a combination of exact diagonalization, Lanczos method (for $q > 1000$, where the flux per hexagonal plaquette is $1/q$ Dirac quanta $\phi_0 = hc/e$), and low-field expansion. For the bulk band structure, we impose doubly periodic (i.e., toroidal) boundary conditions in the (x, y) plane, while to study edge (surface) states we impose singly periodic (i.e., cylindrical) boundary conditions. For $q > 20$ the Hofstadter broadening becomes negligible and the band energies as a function of k_x become nondispersive, corresponding to the real situation in which the magnetic field splitting is small compared to the in-plane hopping amplitude.

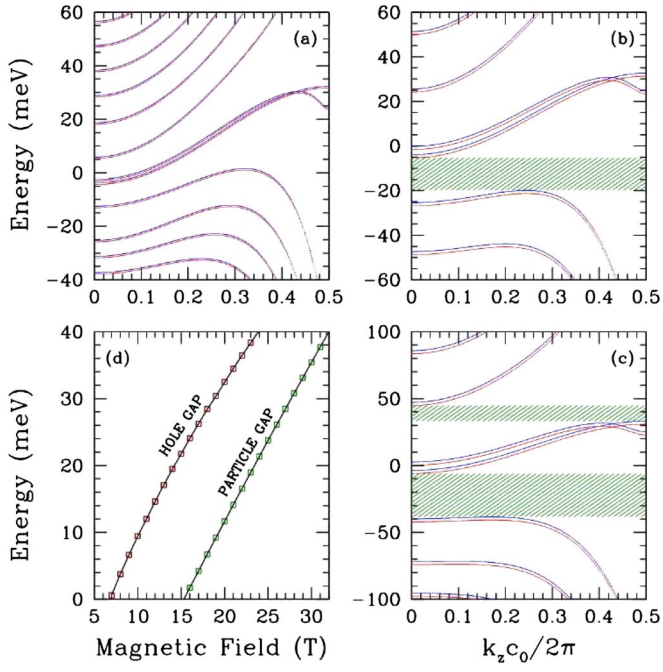

FIG. 4 (color online). Clockwise from upper left: (a) $B = 5$ T, no gap present in the full spectrum. (b) $B = 12$ T, clear gap in the hole LL spectrum. (c) $B = 20$ T clear gaps for both hole and electron LL. Spin-up (blue line) and spin-down (red line) bands are shown. (d) Principal energy gaps surrounding $n = 0$ LLs, including effects due to Zeeman splitting. The particle gap collapses at $B_c^e = 15.4$ T and the hole gap at $B_c^h = 7.0$ T. All energies have been shifted upward by 100 meV.

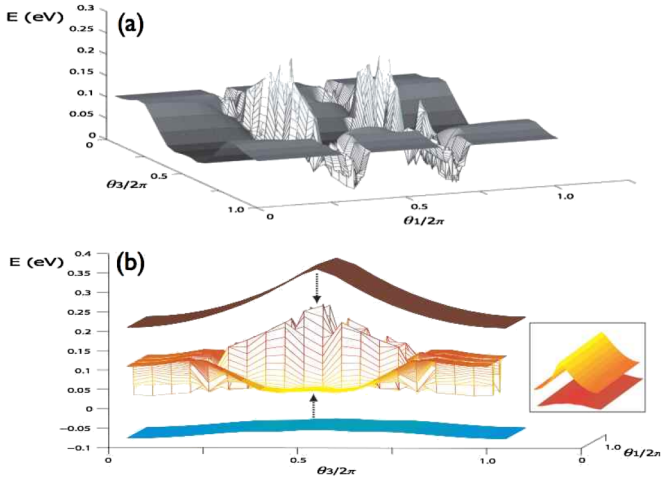

FIG. 5 (color online). Zero mode, first electron Landau level, and surface state spectrum over the first Brillouin zone for one spin species at $B = 40$ T. (a) Surface state spectrum, (b) surface state and bulk $n = 0, 1$ Landau levels where the $n = 1 (n = 0)$ levels are shifted by $+0.1$ eV (-0.1 eV) for clarity. (Inset) $n = 0, 1$ Landau levels unshifted without surface states.

We observe the following characteristics of the spectrum. The zero mode has a dispersion of 40 meV in the low-field limit. The first LL, however, disperses strongly as a function of k_z and for each value of q we scan the energy $E(k_z)$ spectrum to look for the smallest gap. Figure 4 shows the bulk Landau level spectrum for $B = 5$, 12, and 20 T, as well as the field dependence of the principal gaps surrounding the central, weakly dispersive $n = 0$ LLs. We find that both gaps are indirect for $B < 30$ T. In Fig. 5 we plot the bulk band and surface state spectrum as a function of k_x and k_z, which proves the existence of gaps and surface states over the entire Brillouin zone. On the Laughlin cylinder, for each value of k_z, we obtain 2 chiral edge states on each of the upper/lower edges of the cylinder. Unlike the low-field bulk LLs, the edge states disperse as a function of k_x and cross the bulk gap to give a Hall conductivity of $\pm 2e^2/hc_0$ per spin, in agreement with the bulk TKNN analysis. We find that the next gap, in which $\pm 6e^2/hc_0$ per spin, opens only above $B \approx 1000$ T. Thus, only one plateau is observable.

At low fields, each LL accommodates $\frac{\sqrt{3}}{2} a_0^2 B/4\phi_0 = 3.16 \times 10^{-6} B$ [T] states per carbon atom. Accounting for the quadruple degeneracy of the LLs (two K points and two spin polarizations), the central $n = 0$ levels will be filled for fields below 20 T at a doping of only 0.025%. For the lowest field for which we predict the effect, the doping is a modest 0.01% which can be achieved by doping with Boron [21]. Unlike in a many-body gap, the Fermi level is not pinned and the width of the LL will be given by the width of the mobility single-particle gap in disordered graphite. Strong disorder leads to wide Hall plateaus and weak disorder to narrow ones [22].

In addition, the chiral surface sheet should exhibit a ballistic, in-plane longitudinal response ($\rho_{xx} \to 0$ as $T \to 0$) as well as remarkable transport properties along the magnetic field direction [10]. In this direction the system is a stable metal with a T-independent resistivity ρ_{zz}, which can be much larger than h/e^2. However, unlike Ref. [10] we do expect the metallic phase to be unstable to very strong disorder and impurity concentrations which levitate bulk extended states above the Fermi level [23].

B. A. B. wishes to thank F. D. M. Haldane for numerous discussions. D. P. A. is grateful to the Condensed Matter Theory group at Stanford University for its hospitality and sabbatical support, and to S.-C. Zhang for discussions.

[1] K. S. Novoselov *et al.*, Nature (London) **438**, 197 (2005).
[2] Y. Zhang *et al.*, Nature (London) **438**, 201 (2005).
[3] B. I. Halperin, Jpn. J. Appl. Phys. Suppl. **26**, 1913 (1987).
[4] H. L. Stormer *et al.*, Phys. Rev. Lett. **56**, 85 (1986).
[5] L. Balicas *et al.*, Phys. Rev. Lett. **75**, 2000 (1995).
[6] S. M. McKernan *et al.*, Phys. Rev. Lett. **75**, 1630 (1995).
[7] J. C. Slonczewski and P. R. Weiss, Phys. Rev. **109**, 272 (1958); J. W. McClure, Phys. Rev. **108**, 612 (1957).
[8] D. R. Hofstadter, Phys. Rev. B **14**, 2239 (1976).
[9] L. G. Johnson and G. Dresselhaus, Phys. Rev. B **7**, 2275 (1973); S. Y. Leung and G. Dresselhaus, Phys. Rev. B **24**, 3490 (1981).
[10] L. Balents and M. P. A. Fisher, Phys. Rev. Lett. **76**, 2782 (1996).
[11] S. Y. Zhou *et al.*, Nature Phys. **2**, 595 (2006).
[12] H. Kempa, P. Esquinazi, and Y. Kopelevich, Solid State Commun. **138**, 118 (2006).
[13] Y. Kopelevich *et al.*, Phys. Rev. Lett. **90**, 156402 (2003).
[14] M. S. Dresselhaus and G. Dresselhaus, Adv. Phys. **51**, 1 (2002).
[15] We have found that 3DQHE exists in rhombohedral graphite as well, which has *ABCABC* stacking (details to be presented in a future publication).
[16] J. W. McClure, Phys. Rev. **119**, 606 (1960).
[17] J. Nilsson, A. H. Castro Neto, F. Guinea, and N. M. R. Peres, Phys. Rev. Lett. **97**, 266801 (2006).
[18] D. J. Thouless, M. Kohmoto, M. P. Nightingale, and M. den Nijs, Phys. Rev. Lett. **49**, 405 (1982).
[19] Earlier calculations for graphite in a large B field, as in Refs. [16,20], did not address the 3DQHE, nor edge states, and generally neglect the parameter t_{BD}, which we find has a significant effect on the critical fields.
[20] Y. Iye *et al.*, Phys. Rev. B **25**, 5478 (1982).
[21] Y. Hishiyama *et al.*, J. Mater. Res. **17**, 75 (2002).
[22] J. T. Chalker and A. Dohmen, Phys. Rev. Lett. **75**, 4496 (1995).
[23] R. B. Laughlin, Phys. Rev. Lett. **52**, 2304 (1984).